

# Radar Signal Recognition Based on Multilayer Perceptron Neural Network

Original Scientific Paper

## Raja Kumari Chilukuri

Department of Electronics and Communication Engineering, Koneru Lakshmaiah Education Foundation, Guntur, Andhra Pradesh 522502, India  
Department of ECE, VNRVJIE, Hyderabad 500090, India  
chrajakumari@gmail.com

## Hari Kishore Kakarla

Department of Electronics and Communication Engineering, Koneru Lakshmaiah Education Foundation, Guntur, Andhra Pradesh 522502, India  
kakarla.harikishore@kluniversity.in

## K Subba Rao

Department of Electronics and Communication Engineering (Retd.), Osmania University, Hyderabad 500007, India  
kakarlasubbarao51@gmail.com

**Abstract** – Low Probability of Intercept (LPI) radars are developed on an advanced architecture by making use of coded waveforms. Detection and classification of radar waveforms are important in many critical applications like electronic warfare, threat to radar and surveillance. Precise estimation of parameter and classification of the type of waveform will provide information about the threat to the radar and also helps to develop sophisticated intercept receiver. The present work is on classification of modulation waveforms of LPI radar using multilayer perceptron neural (MLPN) network. The classification approach is based on the following two steps. In the first step, the waveforms are analysed using cyclostationary technique which models the signal in bi-frequency (BF) plane. Using this algorithm, the BF images of the signals are obtained. In the second step, the BF images are fed to a feature extraction unit to get the salient features of the waveform and then to the multilayer perceptron neural (MLPN) network for classification. Nine types of noise free modulation waveforms (Frank, four polyphase codes and four poly time codes) are classified using the images obtained in the first step. The success rate achieved is 100 % for noise free signals. The experiment is repeated for various noise levels up to -12dB SNR. The noisy signals, before feeding to the MLPN network, are denoised using two types of denoising filters connected in cascade and the classification success rate achieved is 93.3% for signals up to -12dB SNR.

**Keywords:** LPI radar, signal recognition, cyclostationary (CS), cyclic autocorrelation function (CACF), spectral correlation density (SCD), Bi-frequency (BF), contour plot, denoising, multilayer perceptron neural (MLPN) network, confusion matrix, Artificial Neural Networks.

## 1. INTRODUCTION

Low Probability of Intercept (LPI) radars are developed on an advanced architecture by making use of specially designed coded waveforms which results in low power. The low power levels of LPI radars yield low probability as a synergetic by product. The detection of LPI radars by hostile intercept receivers is highly challenging owing to wide frequency bands and very low peak power. The interception and measurement of LPI signals in hostile radiometric receivers is a difficult task. Recent work has been focused on the early detection of LPI radar signals to defend against an eventual attack [1, 2]. Unfortunately, interception alone cannot

resolve the issue. It is crucial to classify the type of radar and link this radar class to such a platform and/or a weapon system in order to completely detect the radar. LPI radars use special type of waveforms and inhibit the non-cooperative receiver from signal interception and detection. The waveforms of LPI radar signals are challenging for standard electronic reconnaissance methods to differentiate precisely due to the characteristics of low power, wide bandwidth, high resolution, frequency change, etc. Identification of LPI radar signals and improving the recognition ability of reconnaissance equipment is the difficult task in electronic warfare [3].

In order for the electronic attack (EA) or electronic support (ES) system to take immediate action against the attacker, precise estimation of parameters is very important. Also understanding the type of waveform will provide information about the threats to the radar. The ability to re-guide and re-transmit without affecting the electronic system is made much easier by the identification of parameters [4]. Development of sophisticated receivers for interception, detection, and analysis of waveforms is possible only by the knowledge of the parameters and the type of the waveform. Technologies like multi-input multi output (MIMO) radar, ES, and EA systems could also be developed with the help of the parameters [5, 6].

In [7], the authors have estimated the modulation parameters of LPI radar using cyclostationary (CS) technique. CS method is very good for the analysis of LPI radar waveforms as these waveforms are periodic. Poly-time coded signals (T1-T4) are analysed and estimated the parameters of all the codes with an accuracy of 94%. It is presumed that the radar signals are free from noise. Initially, the time domain signals are transformed into bi-frequency (BF) domain using CS techniques and the spectral correlation density (SCD) function is computed. From the contour plot of the SCD function, the parameters of the radar signal are manually extracted and the results are found to be good. But generally, the received signal is corrupted with lot of noise, thereby decreasing the detection or measurement efficiency [8,9]. But by preprocessing the noisy signal using denoising filters, the measurement accuracy could be improved.

In [10], the authors have analysed the radar signals and assessed the parameters of noisy signals using CS techniques. Two different kinds of denoising filters are stacked in cascade to pre-process the noisy waveforms and to improve the signal quality. The denoised waveforms are analysed using CS algorithm and the coefficients of the SCD function are evaluated. Modulation parameters of 9 types of waveforms (Frank,  $P_1$ - $P_4$  and  $T_1$ - $T_4$ ) are extracted with an accuracy of 95% up to -12 dB signal to noise ratio (SNR). The process of identifying the radar type and related missiles can be made after classification and parameter extraction. Most of the existing classification techniques are based on time-frequency (TF) images.

In [6], Choi-William's distribution (CWD) is employed to analyse the signals, and the extracted features from TF images are fed to the Elman neural network (ENN) for classification. The overall success rate (SR) achieved is 94.7% at -2 dB SNR. The authors have analysed 8 types of modulation signals (P1-P4, Frank, LFM, BPSK, and Costas). In [11], the authors used Alex net and classified 10 types of radar signals up to -6 dB SNR and achieved 92.5% success rate.

In [12], the authors have used improved MLPN network on original radar signal and achieved the classification success rate of more than 90% when the SNR is 0 dB. The success rate decreases to about 80% when

the SNR is -5 dB. In [13], the authors employed multiple features images joint decision (MFIJD) model to extract the pixel feature and to get the feature image of the LPI radar signal. The model is created by fusing the original signal, double short-time autocorrelation feature image, and short-time autocorrelation feature image. The TF images are simultaneously fed to the hybrid model classifier and achieved an overall SR of 87.7% at -6dB SNR for 11 types of radar signals.

In [14], the authors have proposed Choi-William's distribution (CWD) to convert radar signals in to time-frequency images. The TF images are simultaneously fed to the automatic modulation classification algorithm based on dense convolutional neural networks (AAMC-DCNN) and achieved an overall success rate of 93.4% at -8dB SNR for 8 types of modulation signals.

In [15], the authors employed Cohen class time-frequency distribution (CTFD) model to extract TF images. 2-D Wiener filtering, bilinear interpolation, and Otsu methods are applied to remove the background noise. The pre-processed TF images are fed to the convolutional neural network (CNN) and achieved an overall success rate of 96.1% at -6 dB SNR for 12 types of modulation signals.

In [9], the authors have developed a model for automatic recognition of modulations of LPI radar signals. Smooth pseudo-Wigner-Ville distribution is used to transform the time-domain signals to TF images. In order to create high dimensional matrices, the TF images are then fed into a triplet convolutional neural network (TCNN) which improves the NW's training process and hence the classifier's ability. Simulation studies showed that the recognition success rate is 94% at -10 dB SNR for 10 signals.

In this paper, a model is developed for automatic recognition of 9 types of radar signal modulations under high noisy conditions. The noisy radar signals are denoised first using two types of denoising filters and the denoised signals are converted into bi-frequency (BF) images using cyclostationary techniques and then the BF images are fed to an MLPN network for classification.

## 2. CYCLOSTATIONARY (CS) ALGORITHM:

Non-stationary signals are effectively analysed using time-frequency algorithms, which can evaluate the signals simultaneously in both time and frequency domains. Many time-frequency (TF) algorithms are discussed in the literature [16]. But cyclostationary (CS) algorithm transforms the signal in to the cycle frequency-frequency domain or bi-frequency (BF) domain. CS method is used here as it is efficient for periodic signals like radar waveforms.

It offers additional properties which are not available in time-frequency domain. The main property of CS is that they have spectral correlation with frequency shifted versions of itself at certain frequency shifts [7]. The

two most important metrics in CS analysis are the cyclic autocorrelation function (CACF) and the spectral correlation density (SCD) functions. The SCD function accurately captures the statistical behavior of the signal in the bi-frequency domain. Many useful characteristics of LPI radar signal can be determined from cyclic auto correlation and the SCD function. It finds applications in many areas like parameter estimation, array processing, signal identification, direction estimation and time of arrival, signal detection [13]. CS is used in detection and identification of weak spread spectrum communication signals. It also offers additional capability in the detection and classification of LPI radar signals [1].

Let the signal to be analyzed be  $x(t)$ . Eq. (1) is used to determine its CACF.

$$R_x^\alpha(\tau) \triangleq \lim_{T \rightarrow \infty} \frac{1}{T} \int_{-T/2}^{T/2} x\left(t + \frac{\tau}{2}\right) x^*\left(t - \frac{\tau}{2}\right) e^{-j2\pi\alpha t} dt \quad (1)$$

where ' $\alpha$ ' represents cycle frequency. The SCD coefficients are computed using eq. (2)

$$\begin{aligned} S_x^\alpha(f) &\triangleq \int_{-\infty}^{\infty} R_x^\alpha(\tau) e^{-j2\pi f \tau} d\tau \\ &= \lim_{T \rightarrow \infty} \frac{1}{T} X\left(f + \frac{\alpha}{2}\right) X_T^*\left(f - \frac{\alpha}{2}\right) \end{aligned} \quad (2)$$

The discrete SCD coefficients of finite signals are evaluated using eq. (3)

$$S_{X_N}^\gamma(n, k) = \frac{1}{N} \sum_{n=0}^{N-1} X_N\left(n, k + \frac{\gamma}{2}\right) X_N^*\left(n, k - \frac{\gamma}{2}\right) \quad (3)$$

where,

$$X_N(n, k) = \sum_{n=0}^{N-1} W(n) x(n) e^{-j2\pi kn} \quad (4)$$

and ' $N$ ' is the length of the signal,  $W(n)$  is the window and ' $\gamma$ ' is the discrete cycle frequency.

SCD is a function of two parameters-cycle frequency and frequency. Fig. 1 shows the block diagram to measure the parameters of noisy radar signals. The input signal is denoised first using two types of denoising filters. The SCD coefficients of the denoised signal,  $x(n)$  are estimated using eq. (3) and the bi-frequency (BF) image of the SCD function is plotted. Fig. 2 shows the BF image of noise free Frank code with a carrier frequency of 1 GHz and the parameters are measured as shown in the Fig. 2. (a) [10].

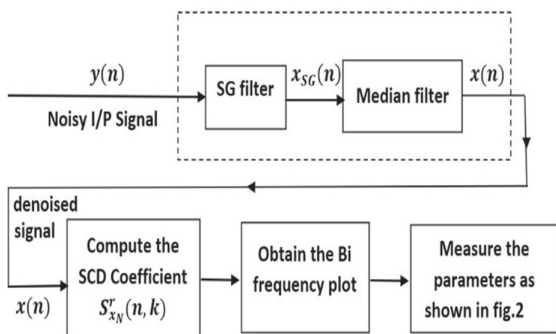
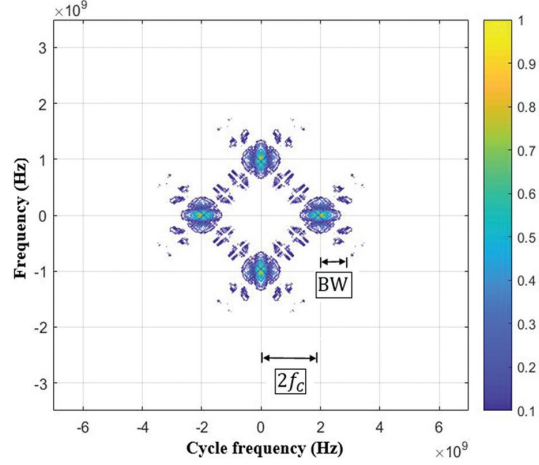
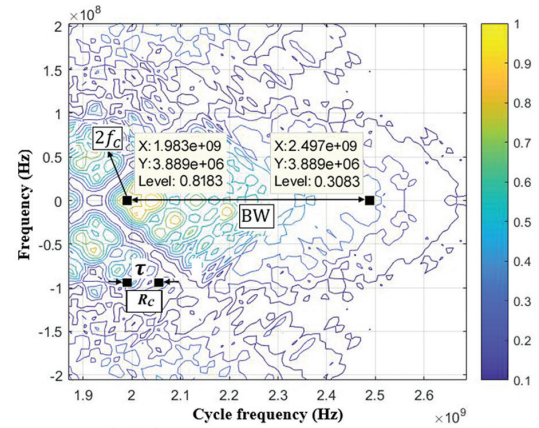


**Fig. 1.** Block diagram of measurement of modulation parameters.

The parameters measured are carrier frequency ( $f_c$ ), bandwidth (BW) and code rate ( $R_c$ ). Contour plots of noise free,  $P_1$  code and  $T_1$  code is shown in Fig. 3 and 4 respectively. From Fig. 2, 3 and 4, it may be observed that the shapes of BF images are different for different types of modulations and these images are the basis for classification of signals.



(a) Complete bi frequency plane



$$f_c = \left(\frac{1.983}{2}\right) \text{GHz}, \text{BW} = (2.497 - 1.98) \text{GHz}, R_c = \frac{1}{\tau}$$

(b) Enlarged version of right most butterfly of Fig. 2 (a)

**Fig. 2.** Contour plot of noise free Frank code for carrier frequency,  $f_c = 1$  GHz

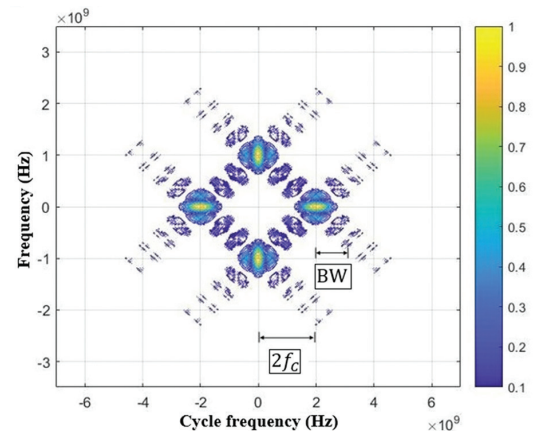


**Fig. 3.** Contour plot of noise free  $P_1$  Code for carrier frequency,  $f_c = 1$  GHz



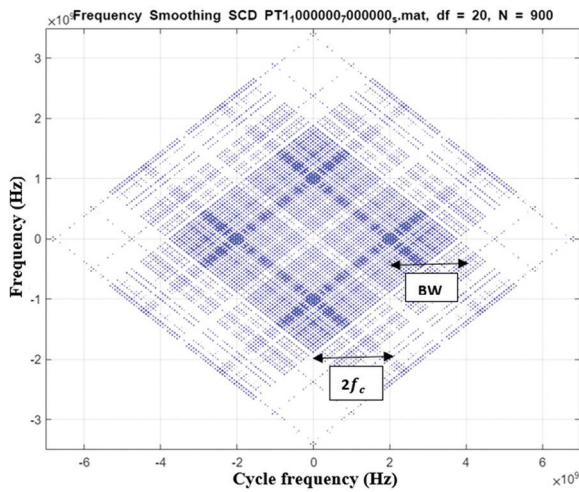


**Fig. 4.** Contour plot of noise free  $T_1$  Codefor carrier frequency,  $f_c=1$  GHz

### 3. FEATURE EXTRACTION USING PRINCIPAL COMPONENT ANALYSIS (PCA):

PCA is one of the dimensionality reduction algorithms used to reduce the class features. It reduces the size of the input data matrix using projection matrix to represent the data in mean square sense. Linear combination of the eigenvectors obtained from the data covariance matrix is used to represent the data in PCA.

The PCA maps an ensemble of  $P$ ,  $N$ -dimensional vectors  $X=[x_1, x_2, x_3, \dots, x_p]$  onto an ensemble of  $P$ ,  $D$ -dimensional vectors  $Y=[y_1, y_2, y_3, \dots, y_p]$ , where  $D < N$ . Using linear transformation one can show that

$$Y = A^H X \quad (5)$$

where  $A$  is a square matrix with  $i$  orthogonal column vectors,  $i=1, 2, \dots, P$  and  $H$  is the Hermitian operation.

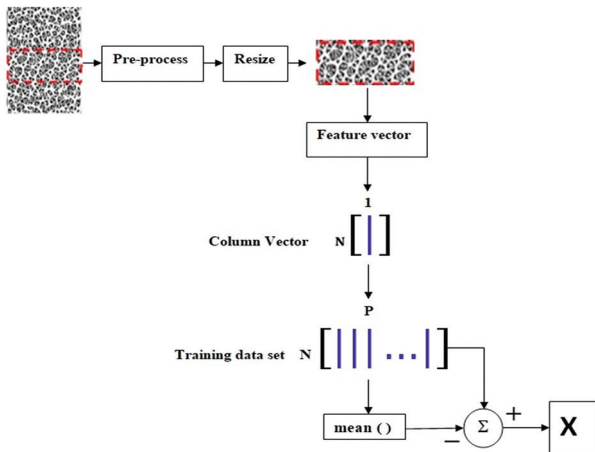


**Fig. 5.** Feature vector generation

The BF images of LPI signals obtained from the CS method are resized to  $60 \times 60$  for all the input signals for pre-processing. In this work a total of  $P=135$  input signals are taken for pre-processing followed by feature extraction process as shown in Fig. 5. Each input signal is represented in column vector and stacked together

to get a matrix of size  $3600 \times 135$ . Later the mean of the training matrix is calculated column wise and the mean is subtracted from the training data set matrix giving the matrix ' $X$ '.  $P$  is the number of training signals and  $N=3600$  is the length of the input vector.  $X$  is of dimension  $3600 \times 135$ . The number of features is reduced from 3600 to  $D=25$ . Hence  $Y$  is of dimension  $25 \times 135$ . Non-zero eigenvectors of  $X$  are obtained using singular value decomposition (SVD) method. SVD states that any  $N \times P$  matrix  $X$  can be decomposed as

$$X = U \Sigma V^H \quad (6)$$

where  $U$  is the  $N \times N$  unitary matrix,  $V$  is the  $P \times P$  unitary matrix and  $\Sigma$  is the matrix of non-negative real singular values. Note that

$$X^H X = V \Sigma^H (U)^H U \Sigma V^H = V (\Sigma^H \Sigma) V^H \quad (7)$$

Equation (7) indicates that the eigenvectors of  $X^H X$  are contained in the ' $V$ ' matrix and the eigenvectors of  $XX^H$  are contained in the ' $U$ ' matrix where ' $U$ ' is given by

$$U = X V \Sigma^{-1} \quad (8)$$

It can be shown that the non-zero eigen values of the higher dimensional covariance matrix  $XX^H$  are computed by computing SVD of smaller dimensional covariance matrix  $X^H X$ . After getting the eigenvector matrix ' $U$ ' and the eigen values from the input data matrix ' $X$ ' using SVD, the transformation matrix  $A$  is obtained from ' $U$ ' using the largest eigen values as shown in Fig. 6. In order to find the largest eigen values a threshold  $Th_\lambda$  is selected and is named as eigenvalue threshold constant. The optimum value of  $Th_\lambda$  is found to be 0.02. Training and testing signals are projected on to matrix  $A$  to get a lower dimensional feature vector with size  $D \times 1$  for one signal. All such signals form a  $D \times P$  matrix and given as input to MLP neural network for classification [17].

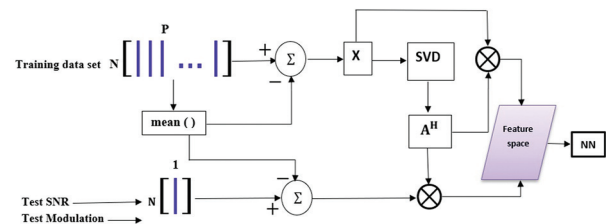


**Fig. 6.** Block diagram of PCA

### 4. CLASSIFICATION NETWORKS

Multilayer perceptron neural (MLPN) network is a feed forward network with an interconnection of non-linear parallel individual computing units. The inputs are propagated layer upon layer in a forward direction resulting in a non-linear mapping of the inputs at the output layer [18].

MLPN network is efficient for small number of hidden layers and also require short training time than deep neural network. The main advantage of MLPN is that it can be used to solve complex non-linear problems and also it makes quick predictions after training. The

same accuracy ratio can be achieved even with smaller samples. Hence MLPN is used for classification of radar signals.

An MLP has three distinctive characteristics:

1. The model of each neuron in the network includes a nonlinear activation function.
2. The network contains one or more layers of hidden neurons that are not part of the input or output of the network.
3. The network exhibits a high degree of connectivity, determined by the synapses of the network.

The MLPN network is represented as

$$y_k(l) = \phi(\sum_{h=1}^H w_{kh} \phi(\sum_{i=1}^I w_{hi} x_i(l))) \quad (9)$$

where  $x_i$  is the input,

$y_k$  is the output,

$i$  is the number of input nodes,

$l$  is the sample number,

$k$  is the output index

and  $h$  is the number of layers.

The weight values between neurons  $i$  and  $k$  and  $i$  and  $h$  are represented as  $w_{kh}$  and  $w_{hi}$  respectively, and the activation function is represented as  $\phi$ . A single global training technique using supervised learning determines all weight values  $w$  in the MLP simultaneously [19]. For distinct layers of neurons, the activation functions can change and is monotonic. As the number of network layers is relatively low, the activation function used is sigmoid function which is defined as:

$$\phi(x) = \frac{1}{(1+e^{-x})} \quad (10)$$

A two-layer feed-forward neural network with one hidden layer and with nine neurons in the output layer, one for each type of modulation, as shown in Fig. 7 is developed for classification of images.

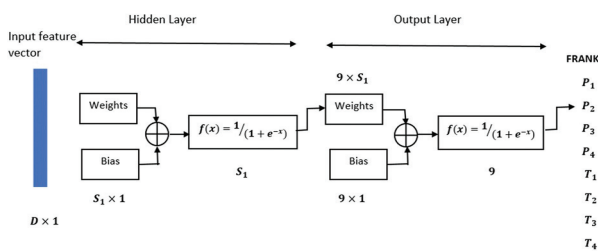


**Fig. 7.** Block diagram of Two-Layer Perceptron Neural Network

For each detection method, the feature vector dimension  $D \times 1$  is obtained using the principal component analysis. The optimum number of neurons is chosen after considering several different numbers for the hidden layer [20]. Supervised training of the MLP network uses the gradient of the performance function to determine the weights. The gradients are determined using back propagation algorithm.

To increase the network's convergence speed of the training algorithms, variable learning rate technique is used. The pace of learning is maintained constant during training using typical steepest decent method. The correct learning rate setting is extremely important for best performance. Network regularization  $R$  is used to improve the network generalization. The network regularization  $R$  is calculated using eq. (11).

$$R = g * M_{SE} + (1-g) \quad (11)$$

where  $M_{SE}$  is the mean sum of square of the network errors and  $g$  is the performance ratio ( $g=0.0197$ ). The regularization performance target was established at  $R=0.9816$ . The best value is selected for each training set using a variety of training iterations (epochs). The size of the weight vector is  $50 \times 25$  since the number of hidden layers are 50 and the number of features is 25.

## 5. SIMULATION RESULTS

The overall block diagram for estimation of parameters and classification of signals is shown in Fig. 8. The BF images obtained from the detector unit are fed to the feature extraction unit and then to the MLPN network for classification.

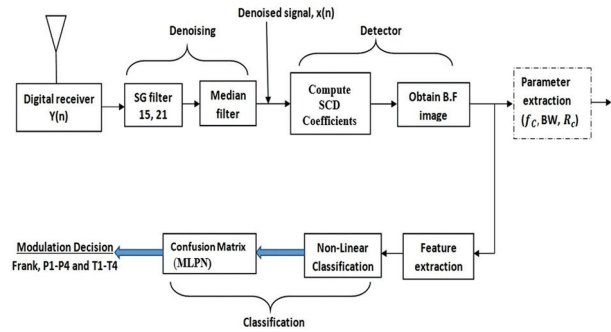


**Fig. 8.** Parameter extraction and classification

Test signals with  $-6$  dB SNR are used for optimization. The optimum selection is based on the highest average probability of correct classification. Nine types of modulation signals (Frank,  $P_1$ - $P_4$  and  $T_1$ - $T_4$ ) are used for classification. The experiment is carried out with three different carrier frequencies (0.8 GHz, 1 GHz and 1.2 GHz). The SNR of each signal is varied from noise free signal to  $-12$  dB instead of 3 dB. Thus, a total of 135 ( $9 \times 3 \times 5$ ) signals are considered. For better training and testing of the two-layer MLPN network, the signals are repeated 216 times. Thus, making the total number of signals to be 29,160. Out of 29,160 signals, 70% of them are used for training, 15% for testing and the remaining 15% for validation. Ten test runs are used to build the classification statistics. To randomize the weight matrices of each test, the networks are reset using the ideal network parameters. The maximum number of epochs (iterations) is kept at 1000. The number of neurons in the hidden layer is varied from 10 to 150 and the optimum number is found to be 50 for high noisy signals. The optimum eigen value threshold constant is found to be 0.02 for noisy signals. Confusion

matrices are generated for the classification test at each SNR level. The classification success rate (SR) is obtained from the confusion matrix.

**Confusion matrix**

Output Class	Frank	72	0	0	0	0	0	0	0	0	0	0	0	0	100%
	P <sub>1</sub>	0	72	0	0	0	0	0	0	0	0	0	0	0	100%
	P <sub>2</sub>	0	0	72	0	0	0	0	0	0	0	0	0	0	100%
	P <sub>3</sub>	0	0	0	72	0	0	0	0	0	0	0	0	0	100%
	P <sub>4</sub>	0	0	0	0	72	0	0	0	0	0	0	0	0	100%
	T <sub>1</sub>	0	0	0	0	0	72	0	0	0	0	0	0	0	100%
	T <sub>2</sub>	0	0	0	0	0	0	72	0	0	0	0	0	0	100%
	T <sub>3</sub>	0	0	0	0	0	0	0	72	0	0	0	0	0	100%
	T <sub>4</sub>	0	0	0	0	0	0	0	0	72	0	0	0	0	100%
			100%	100%	100%	100%	100%	100%	100%	100%	100%	100%	100%	100%	100%
		Frank	P <sub>1</sub>	P <sub>2</sub>	P <sub>3</sub>	P <sub>4</sub>	T <sub>1</sub>	T <sub>2</sub>	T <sub>3</sub>	T <sub>4</sub>					
		Target Class													

**Fig. 9.** Confusion matrix of noise free signals

**Confusion matrix**

Output Class	Frank	1728	0	0	0	0	0	0	0	0	0	0	0	0	100%
	P <sub>1</sub>	0	1728	0	0	0	0	0	0	0	0	0	0	0	100%
	P <sub>2</sub>	0	0	1728	0	0	0	0	0	0	0	0	0	0	100%
	P <sub>3</sub>	0	0	0	1728	0	0	0	0	0	0	0	0	0	100%
	P <sub>4</sub>	0	0	0	0	1728	0	0	0	0	0	0	0	0	100%
	T <sub>1</sub>	0	0	0	0	0	1728	0	0	0	0	0	0	0	100%
	T <sub>2</sub>	0	0	0	0	0	0	1536	0	0	0	0	0	0	100%
	T <sub>3</sub>	0	0	0	0	0	0	0	1536	0	0	0	0	0	100%
	T <sub>4</sub>	0	0	0	0	0	0	0	0	1536	0	0	0	0	100%
			100%	100%	100%	100%	100%	88.9%	88.9%	88.9%	88.9%	96.3%	3.7%		
		Frank	P <sub>1</sub>	P <sub>2</sub>	P <sub>3</sub>	P <sub>4</sub>	T <sub>1</sub>	T <sub>2</sub>	T <sub>3</sub>	T <sub>4</sub>					
		Target Class													

**Fig. 10.** Confusion matrix for signals up to -6dB

**Table 2.** Comparison of the results with the literature values.

S. No (1)	Reference number (2)	Type of TF/BF algorithm used (3)	Type of Network used (4)	No. of modulation signals used (5)	Max. noise level SNR (dB) (6)	Success rate (SR) (7)
1	[10], Oct. 2016	Choi-Williams distribution (CWD)	Elman neural network (ENN)	8	-6	92.5%
2	[19], Aug. 2018	Cohen class time-frequency distribution (CTFD)	Convolutional neural networks (CNN)	12	-6	96.1%
3	[12], 2019	Original Radar signal	Improved MLPN	7	0	90%
4	[6], Jan.2020	Multiple feature images joint decision (MFJJD)	Hybrid model classifier	11	-6	87.7%
5	[18], Jan. 2021	Choi-Williams distribution (CWD)	Dense convolutional neural networks (DCNN)	8	-8	93.4%
6	[9], Nov. 2021	Smooth pseudo-Wigner-Ville distribution (WVD)	Triplet convolutional neural network (TCNN)	10	-10	94.7%
7	Proposed method	Cyclostati-onary technique	Multilayer perceptron neural network (MLPN)	9	-12	93.3%

It is found that the classification success rate is 100% for noise free signals when the numbers of hidden layers are 10. Fig. 9 shows the confusion matrix of noise free signals. The experiment is repeated for various noise levels up to -12 dB in steps of 3 dB. Figs. 10 and 11 show the confusion matrices of noisy signals up to -6 dB and -12 dB respectively.

**Confusion matrix**

Output Class	Frank	3240	0	0	0	0	0	0	0	0	0	0	0	0	100%
	P <sub>1</sub>	0	3240	0	0	0	0	0	0	0	0	0	0	0	100%
	P <sub>2</sub>	0	0	2592	0	0	0	0	0	0	0	0	0	0	100%
	P <sub>3</sub>	0	0	0	3240	0	0	0	0	0	0	0	0	0	100%
	P <sub>4</sub>	0	0	0	0	3240	216	432	432	216	62.5%				
	T <sub>1</sub>	0	0	0	0	0	3024	0	0	0	100%				
	T <sub>2</sub>	0	0	0	0	0	0	2808	0	0	100%				
	T <sub>3</sub>	0	0	0	0	0	0	0	2808	0	100%				
	T <sub>4</sub>	0	0	0	0	0	0	0	0	3024	100%				
			100%	100%	80.0%	100%	100%	93.3%	86.7%	86.7%	93.3%	3.7%			
		Frank	P <sub>1</sub>	P <sub>2</sub>	P <sub>3</sub>	P <sub>4</sub>	T <sub>1</sub>	T <sub>2</sub>	T <sub>3</sub>	T <sub>4</sub>					
		Target Class													

**Fig.11.** Confusion matrix for signals upto -12dB

**Table 1.** Classification results of various noisy signals

Noise level of the signal (1)	No. of hidden layers (2)	Success rate (SR) (3)
Noise free signals only	10	100%
Upto-3 dB SNR	10	96.3%
Upto-6 dB SNR	10	96.3%
Upto-9 dB SNR	10	94.4%
Upto-12 dB SNR	50	93.3%



Table. 1 shows the classification results for various noisy signals. Column 1 shows the maximum noise level. Column 2 shows the maximum number of hidden layers considered and the last column shows the classification success rate. The success rate achieved for signals up to -6 dB SNR is 96.3%. The maximum classification success rate achieved for signals up to -12 dB SNR is 93.3% and the number of hidden layers is 50.

Table. 2 shows the comparison of the results with the literature values. Column 1 shows the serial number. Column 2 shows the reference number and month and year of publication. Column 3 shows the type of algorithm used to get the TF/BF image and column 4 gives the type of neural network used. Columns 5 and 6 show respectively the maximum number of modulation signals and the maximum SNR considered. The last column shows the classification success rate achieved. For S. No. 2, though the success rate is the highest (96.1%), the noise level considered is only up to -6 dB SNR. The next highest success rate is 94.7% for S. No. 5 and the noise level considered is also less (-10 dB SNR). For the proposed method, the success rate achieved is 93.3% with the noise level considered up to -12 dB SNR. It means even for high noisy signals (compared to S. No. 5), the success rate achieved is nearly same. Hence the proposed method is superior.

## 6. CONCLUSIONS

Detection and classification of radar waveforms are important in many critical applications like electronic warfare, threat to radar and surveillance. LPI radar waveforms are classified using cyclostationary techniques and multilayer perceptron neural (MLPN) network. The main advantage of MLPN is that it can be used to solve complex non-linear problems and also it makes quick predictions after training. The classification process is carried out in three steps. Firstly, the noisy signals are denoised using denoising filters. Later the signals are analysed using cyclostationary algorithm and the BF images are obtained. In the third step, the images are fed to the MLPN network for classification. Nine types of modulation waveforms are considered under various noise conditions up to -12 dB SNR. Before feeding to the MLPN network for classification, the BF images are fed to the feature extraction unit to reduce the number of features to 25. With the proposed method, the classification success rate achieved is 100% for noise free signals. But as the noise level increases, the success rate decreases. The maximum success rate achieved is 93.3% for signals up to -12 dB SNR. When compared with literature values, the proposed method is better as the classification success rate is good even in low SNR conditions.

## 7. ACKNOWLEDGEMENT:

The authors express their sincere thanks to the management and principal, Vallurupalli Nageswara Rao Vignana Jyothi Institute of Engineering and Technology, Hyderabad for providing necessary facilities to carry out this work.

## 8. REFERENCES

- [1] P. E. Pace, "Detecting and classifying low probability of intercept radars", 2<sup>nd</sup> Edition, Norwood: Artech House, 2009.
- [2] M. I Skolnik, "Introduction to radar systems", 3<sup>rd</sup> Edition, McGraw-Hill Education, New York, 2003.
- [3] W. Si, J. Luo, Z. Deng, "Radar Signal Recognition and Localization Based on Multiscale Lightweight Attention Model", *Journal of Sensors*, Vol. 2022, 2022, pp. 1-13.
- [4] M. S. Sunder, K. Subbarao, "Cyclostationary Analysis of Polytime Coded Signals for LPI Radars", *International Journal of Research in Engineering and Technology*, Vol. 4, No. 6, 2015, pp. 544-560.
- [5] J. E Fielding, "Polytime coding as a means of pulse compression", *IEEE Transactions on Aerospace and Electronic Systems*, Vol. 35, No. 2, 1999, pp. 716-721.
- [6] M. Zhang, L. Liu, M. Diao, "LPI Radar Waveform Recognition Based on Time-Frequency Distribution", *Sensors*, Vol. 16, No. 10, 2016, pp. 1-20.
- [7] R. K. Chilukuri, H. Ki. Kakarla, K. Subbarao, "Estimation of Modulation Parameters of LPI Radar Using Cyclostationary Method", *Journal of Sensing and Imaging*, Vol. 21, No. 51, 2020, pp.1-20.
- [8] T. R. Kishore, K. D. Rao, "Automatic Intrapulse Modulation Classification of Advanced LPI Radar Waveforms", *IEEE Transactions on Aerospace and Electronic Systems*, Vol. 53, No. 2, 2017, pp. 901-914.
- [9] L. Liu, X. Li, "Radar signal recognition based on triplet convolutional neural network", *EURASIP Journal on Advances in Signal Processing*, 2021, pp. 1-16.
- [10] R. K. Chilukuri, H. K. Kakarla, K. Subbarao, "Estimation of intra pulse modulation parameters of LPI radar under noisy conditions", *Journal of International Journal of Microwave and Wireless Technologies*, Vol. 14, No. 9, 2022, pp. 1177-1194.
- [11] G. Limin, C. Xin, "Low Probability of Intercept Radar Signal Recognition Based on the Improved Alex Net Model", *Proceedings of the 2nd International Conference on Digital Signal Processing*, Tokyo, Japan, 25-27 February 2018, pp. 119-124.

- [12] F. Li, Y. Wang, L. Zhao, Z. Yang, "Radar modulation recognition based on MLP neural network", Proceedings of the International Conference on Microwave and Millimeter Wave Technology, Guangzhou, China, 13 February 2020, pp. 1-3.
- [13] Z. Ma, Z. Huang, A. G. Huang, "LPI Radar Waveform Recognition Based on Features from Multiple Images", *Sensors*, Vol. 20, No. 2, 2020, pp. 1-23.
- [14] W. Si, C. Wan, C. Zhang, "Towards an accurate radar waveform recognition algorithm based on dense CNN", *Multimedia Tools and Applications*, Vol. 80, No. 2, 2021, pp. 1779–1792.
- [15] Z. Qu, X. Mao, Z. Deng, "Radar Signal Intra-Pulse Modulation Recognition Based on Convolutional Neural Network", *IEEE Access*, Vol. 6, 2018, pp. 43874-43884.
- [16] X. Zhang et al. "Radar Signal Intra pulse Modulation Recognition Based on a Denoising-Guided Disentangled Network", *Remote Sensing*, Vol. 14, No. 5, 2022, pp. 1-15.
- [17] T. Farrell, G. Prescott, "A Method for Finding Orthogonal Wavelet Filters with Good Energy Tiling Characteristics", *IEEE Transactions on Signal Processing*, Vol. 47, No. 1, 1999, pp. 220-223.
- [18] M. Shyamsunder, "Classification and estimation of modulation parameters of LPI Radar signals", Osmania University, Hyderabad, India, Ph.D. thesis, 2020.
- [19] Z. Ma, W. Yu, P. Zhang, Z. Huang, A. Lin, Y. Xia, "LPI Radar Waveform Recognition Based on Neural Architecture Search", *Computational Intelligence and Neuroscience*, Vol. 2022, 2022, pp. 1-15.
- [20] Q. Guo, X. Yu, G. Ruan, "LPI Radar Waveform Recognition Based on Deep Convolutional Neural Network Transfer Learning", *Symmetry*, Vol. 11, No. 4, 2019, pp. 1–14.